Magnetic and energetic properties of low-index Cr surfaces and Fe/Cr interfaces: A first-principles study

R. Soulairol,[1] Chu-Chun Fu,[1] and C. Barreteau[2]
[1]*CEA, DEN, Service de Recherches de Métallurgie Physique, F-91191 Gif-sur-Yvette, France*
[2]*CEA Saclay, IRAMIS, SPCSI, F-91191 Gif-sur-Yvette Cedex, France*
(Received 1 August 2011; published 5 October 2011)

Density functional theory calculations are performed to investigate the impact of magnetism on the energetics of low-index Cr surfaces and Fe/Cr interfaces, that is, Cr(100), Cr(110), Fe/Cr(100), and Fe/Cr(110). We have also determined the stability of various Cr magnetic structures, particularly the spin-density waves, in the presence of these surfaces and interfaces. We show that the most stable structure of the spin-density wave is mainly dictated by the subtle balance between bulk and surface/interface influences, and strongly dependent on the surface/interface orientation. Regarding the Cr surfaces, we confirm the role of magnetism to lower the surface energy of Cr(100) with respect to Cr(110). Among all the possible orientations of the wave vector, only the out-of-plane wave is found to be stable near Cr(100) surfaces with the high-moment sites located at the surface layer. At variance, the in-plane wave is shown to be the most stable one, consistent with experimental data for very thin Cr(110) films. Concerning the Fe/Cr interfaces, magnetic frustrations are identified to be responsible for a higher formation energy of Fe/Cr(110) compared to that of Fe/Cr(100). This unusual anisotropy of interface energies is clearly different from the corresponding interfaces between Cr and a nonmagnetic element, Cu. Two ways are suggested to relax partially the magnetic frustrations at the (110) interface and to lower its formation energy. Noncollinear magnetic configurations can be developed where local moments of Fe and Cr atoms are perpendicular to each other. Also, in order to preserve phase coherence, in-plane spin-density waves show a very stable magnetic structure with the nodes at the interface layer. The presence of low-moment sites at Fe/Cr(110) offer another way to relax the magnetic frustrations and lower the interfacial energy.

DOI: 10.1103/PhysRevB.84.155402 PACS number(s): 71.15.Mb, 71.20.Be, 71.15.Nc, 75.70.Rf

I. INTRODUCTION

Cr is used for many technological applications in materials design. In particular, it is widely considered as a key alloying element of steels. For instance, in the specific field of nuclear-materials development, Cr is a major component of ferrito-martensitic steels which contributes to improve materials resistance to corrosion, irradiation, and swelling. Besides, during the last decades, Fe/Cr multilayers have been shown to exhibit giant magnetoresistance with potential application for electronic devices.

On the other side, Cr still triggers significant research efforts due to its magnetic properties. For instance, as observed experimentally, the magnetic ground state of Cr consists in a so called incommensurate spin-density wave (SDW), that is, a long-period modulation of the magnitude of local moments along ⟨100⟩ directions, where nearest-neighbor atoms show antiparallel coupling.[1,2] This magnetic arrangement, stable up to the Néel temperature ($T_{\text{Néel}} = 311$ K) in pure Cr, has been proposed to be a direct consequence of the nesting properties of Cr Fermi surface.[3] Its stability is therefore very sensitive to any modification of the electronic structures caused by, for example, the presence of defects.[3,4] In the perfect Cr bulk, the SDW is characterized by a multi-$\vec{q}$ state ($\vec{q}$ denotes the wave vector), that is, magnetic domains with SDWs oriented along the various ⟨100⟩ directions may coexist. These domains are however expected to be no longer equivalent close to extended defects such as surfaces and interfaces, leading to the formation of a single-$\vec{q}$ state.[5] Interaction between these defects and the magnetic structure of Cr is a real concern of the last decades, motivated by the high interest on the Cr thin films.

Experimentally, both neutron and x-ray diffraction[6] and scanning tunneling microscopy[7–10] studies have established the presence of the SDW near Cr surfaces at temperatures ranging from 6 to 300 K. These data also pointed out the influence of surface orientation favoring SDWs with specific wave vectors. Close to a (100) surface, the wave vectors clearly prefer to be perpendicular to the surface.[5,6,9] However, the conclusion concerning the SDW orientation near a (110) surface is much more controversial.[7,10,11] In addition, other features of the SDW as its polarization state (longitudinal versus transversal) and the corresponding spin-flip transition temperature (T_{sf}) are also submitted to surface influence.[9,12,13] Besides the SDW structure, thin films of Cr also exhibit, at variance with bulk Cr, interesting high-temperature appearance of the antiferromagnetic state coupled with an increase of the Néel temperature.

It is worth mentioning that for accurate theoretical simulations explicit consideration of both extended defects and the SDW is a nontrivial task. Due to the long period of the latter, such studies often require very large simulation cells. Also, density functional theory (DFT) calculations predict either the antiferromagnetic (AF) or the nonmagnetic (NM) to be the ground state of the perfect bcc Cr, depending on the exchange-correlation functional used.[14,15] The experimental magnetic ground state, which can only be approximated by a commensurate SDW due to the periodic-boundary conditions, is rather a metastable state, a few milli-electron volt per atom higher in energy than the (100)-layered AF state. Therefore, many previous DFT calculations on Cr surfaces have rather neglected the experimentally observed SDW to focus on the simpler AF phase. For instance, Ossowski *et al.*[16]

compared the (100) and (210) surfaces and enlightened that the magnetism was responsible for an overstabilization of the Cr(100). This result was also consistent with previous data from Alden *et al.*[17] predicting, by means of a tight binding model, a stability inversion between the Cr(100) and the Cr(110) due to magnetic effects. However, very little is known theoretically about the SDW structures near the Cr surfaces so far. To our knowledge, only a few previous DFT studies have considered the SDW structures near Cr(100) surfaces.[18–20] Besides, Ossowski *et al.*[21] has reported a modulation of local magnetic moments near another extended defect in Cr, that is, a $\Sigma 5(210)$ grain boundary. This modulation has been interpreted as a spontaneous creation of SDWs due to the presence of the grain boundary.

Concerning FeCr systems, many experimental efforts have been devoted to the study of FeCr multilayers, motivated by their giant magnetoresistance. For (100) multilayers, the stability and polarization of the SDWs according to perturbed angular correlation spectroscopy[12] and neutron scattering[22] come to be directly linked to the thickness of the Cr slab. The SDW phase only appears beyond a critical thickness of around 45 Å, close to the typical value of the SDW period (60 Å), the AF phase being observed below this limit.[23] The interplay between Cr-Cr, Fe-Fe, and Fe-Cr magnetic coupling may also induce the appearance of noncollinear structures such as helical SDW. They appear when successive Fe slabs separated by Cr show slightly tilted magnetization directions.[23,24] For (110) multilayers, SDW structure has also been observed by neutron diffraction for rather thick Cr slabs (260 Å).[25,26] In such structures, the orientation of Cr local moments is also affected by the magnetization direction of neighboring Fe layers with a perpendicular pinning of Fe and Cr magnetic moments.[25,26]

Theoretically, the (100) Fe/Cr multilayers have been extensively studied. It was shown that the periodicity of SDWs was not any more a direct consequence of Fermi surface nesting as in the bulk, but mainly governed by the boundary conditions.[18,27] Although precise value of the AF versus SDW transition thickness varies with calculation technique, it has been shown, in agreement with experiments, that AF structure was favored for very thin Cr slabs ($N_{\mathrm{Cr}} \lesssim 24$ atomic layers). A further increase of Cr thickness causes the creation of SDW nodes and induces "magnetic phase slips" that have been observed experimentally.[28] However, the corresponding SDW period was observed to be significantly different to the bulk value.[18,24,27,29]

From another point of view, the present study will rather focus on the properties of the Fe/Cr interfaces themselves, which are of crucial interest to describe the energetics and the structures of α coherent precipitates of Cr which may appear in α-Fe when Cr concentration exceeds around 10%.[30,31]

Previous experimental works have shown that magnetic frustrations may occur due to the presence of the interface, revealed by a decrease of local magnetic moment near perfect (110) interfaces.[32] Similar phenomenon has also been mentioned near a (100) interface, but it has rather been connected to the presence of defective interfaces showing atomic steps.[22]

Theoretically, although the role of magnetism on the energetics of the interfaces has only been studied by DFT assuming the AF phase of Cr,[33,34] more realistic interfaces including inter-diffusion and atomic steps have already been proposed by means of tight binding[35–38] and periodic Anderson models[39–41] to induce long-ranged magnetic structures in either Fe or Cr slabs.

In this study we aim, by means of DFT calculations, at drawing a clearer picture of the interplay between extended defects (Cr surfaces and Fe/Cr interfaces) and various magnetic structures including the SDWs. Section II of this paper describes the calculation methods. The energetics and magnetic structures of the low-index (100) and (110) surfaces with SDWs are presented in detail in Sec. III A. Section III B is devoted to the (100) and (110) interfaces between Fe and Cr, focusing particularly on the role of Cr magnetism on the anisotropy of interfacial energies. The case of perfect (100) and (110) interfaces showing collinear and noncollinear configurations are discussed in Secs. III B 1 and III B 2, respectively. Finally, we describe in Sec. III B 3 the SDW structures in the presence of Fe/Cr interfaces.

II. METHODOLOGY

The present calculations have been performed within the density functional theory as implemented in the SIESTA code.[42] This localized-basis-set DFT approach has been proved to give reliable results on the energetics and magnetic structures in pure Fe and Cr,[43] and in the SDW-Cr containing defects,[4] compared with more robust plane-wave codes within projector augmented wave (PAW)[14] and all electrons approaches.[15]

All our calculations are spin polarized. The implementation of noncollinear magnetism[44] has also been used in the particular case of Fe/Cr interface calculations. Spin-orbit coupling effects are not included, thus, possible effects of polarization state of SDW are neglected. All results are obtained within the generalized gradient approximation (GGA) for the exchange-correlation functional in the Perdew-Burke-Ernzerhof (PBE) form.

Concerning other DFT approximations, core electrons are replaced by nonlocal norm-conserving pseudopotentials while valence electrons are described by linear combination of numerical pseudoatomic orbitals (LCAO) within the SIESTA code. The pseudopotentials and the basis sets for Cr, Fe, and Cu atoms are the same as used in Refs. 4, 43, and 45, where they have shown to be accurate enough concerning the relevant energetic and magnetic properties.

The k-point grids used for different supercells vary with the corresponding number of atoms. They have been chosen to achieve an equivalent k-space sampling to a cubic unit cell for a bcc lattice with a $12 \times 12 \times 12$ shifted k grid. Calculated surface and interface formation energies have been verified to be well converged with regard to these grids.

The Methfessel-Paxton broadening scheme with a 0.3 eV width are used as in our previous works.[4,43] We have performed constant pressure calculations, that is, the structures are optimized by relaxing both the atomic positions and the shape and volume of the supercell. In particular, all the pressures in the direction perpendicular to surface or interface planes has been verified to be less than 3 kbar.

TABLE I. Relaxed and unrelaxed Cr surface formation energies (E^f_{surf} in J/m^2) by SIESTA as a function of magnetic state of Cr. All the values shown with AF- and NM-Cr are converged with respect to the thickness of the Cr slab, as well as for the Cr(100) with out-of-plane (op) SDWs. The corresponding number of atomic layers at both AF and NM states is 14, whereas for Cr(100) with SDW we have considered 28, 56, and 84 atomic-layer cells. For the Cr(110) surface with in-plane (ip) SDW, a supercell of 14 atomic layers has been used with 28 atoms per layer.

Cr magnetic state	AF	NM	1 op-SDW	2 op-SDW	3 op-SDW	ip-SDW
Relaxed						
(100)	3.37	4.20	3.40	3.39	3.39	–
(110)	3.44	3.64	–	–	–	3.49
Unrelaxed						
(100)	3.38	4.34	3.42	3.42	3.42	–
(110)	3.44	3.71	–	–	–	3.53

Supercell calculations were performed to study the properties of both surfaces and interfaces. Concerning the surface calculations, each slab contains two surfaces and shows two-dimensional periodic boundary conditions (PBC). We considered for each calculation at least 10 Å of vacuum to separate the slabs in order to prevent from a direct surface-surface interaction. Concerning the interfaces, the bicrystal approximation with three-dimensional PBC was used. The simulation cell contains therefore two identical Fe/Cr interfaces. Within this study we consider perfect surfaces and interfaces, that is, effects of possible surface reconstruction, steps and interdiffusion are thus beyond the scope of this work.

In all the calculations with the simple magnetic phases (AF or NM-Cr), Cr slabs ranging from 14 to 39 atomic layers have been considered to ensure the convergence of the surface or interface formation energies. For the lateral dimensions of the supercells, we have considered one and two atoms per layer for, respectively, the (100) and (110) surface/interface.

To include the SDWs near the surface/interface, we have considered a SDW of 14 times the lattice constant (a_0) with $\vec{q}^{\,\text{SDW}} = 0.929$, where the experimental value of $\vec{q}^{\,\text{SDW}}$ in bulk Cr is around 0.95. This choice is a reasonable compromise between the computational cost and an accurate description of SDW properties. For these cases we considered various slab thicknesses from 1 to 3 SDW periods. The lateral dimensions were the same as for the AF-Cr case, except for SDWs near the (110) surface/interface, which required extended lateral dimensions, up to $14a_0$.

We have also performed some complementary DFT calculations carried out with quantum-espresso package,[46] in order to confirm the accuracy of our SIESTA results on Fe/Cr interfaces. Within the PWSCF calculations we used the same ultrasoft pseudopotentials as in Ref. 43 and a plane wave basis set with a 30 Ry energy cutoff.

III. RESULTS AND DISCUSSIONS

A. Influence of magnetism on the energetics of Cr surfaces

In this section we consider the (100) and (110) surfaces in presence of various representative magnetic structures of Cr: from the AF and the NM state to the SDW with different orientations with respect to the surfaces.

The corresponding surface formation energies per unit area (E^f_{surf}) are calculated as follows:

$$E^f_{\text{surf}} = \frac{1}{2A}[E(\text{Cr}_N,2\text{surf}) - E(\text{Cr}_N)], \quad (1)$$

where $E(\text{Cr}_N,2\text{surf})$ denotes the total energy of a N-layer bcc Cr slab with two identical surfaces. $E(\text{Cr}_N)$ is the total energy of a bcc Cr bulk cell with the same number of Cr atoms and magnetic state. A is the area of the surface which is equal to a_0^2 and $\sqrt{2}a_0^2$ for (100) and (110) surfaces, respectively.

First of all, in order to reveal the significant impact of magnetism on the energetics, we compare the surface formation energies of Cr at the AF and the NM states. Cr slabs of 14 atomic layers parallel to the surface are used for such calculations. The energetics of these low-index Cr surfaces may be a subtle balance between the surface-atom coordination and the magnetism. Indeed, based on a "number of broken-bonds" argument, the energetically most favorable surface for the NM-Cr is expected to be the densest surface, that is, the (110), as in other nonmagnetic bcc metals. However, when switching on the magnetism, the usual anisotropy of the surface energies comes to be reversed, Cr(100) being now lower in energy than Cr(110). The respective surface energies are 3.37 and 3.44 J/m^2 for the AF state (Table I). Our results confirm this effect to be driven by magnetism. As shown in Fig. 1, this reversal is associated to a particularly strong increase of Cr local magnetic moments near the Cr(100) surface. This finding is in qualitative agreement with previous results using a tight-binding LMTO approach,[17] although the surface energy of Cr(100) from our study is closer to the DFT-PAW value of 3.25 J/m^2 from Ref. 16.

By checking the projected density of electronic states (PDOS) plotted in Fig. 2, we notice the presence of a huge peak at the Fermi level (E_F) of the topmost-layer Cr PDOS corresponding to the NM-Cr(100) surface, which is clearly reduced when switching from the NM to the AF Cr. At variance, magnetism appears to induce weaker changes in the PDOS of the topmost-layer Cr atoms for the (110) surfaces. These observations are consistent with the magnetically driven energy reversal between the (100) and the (110) surfaces.

It is interesting to mention that similar surface states appear at the Fermi level not only in the perfect unreconstructed (100) surface of NM-Cr, but also of Mo and W, belonging to the same group VI of the Periodic Table. The difference is that while

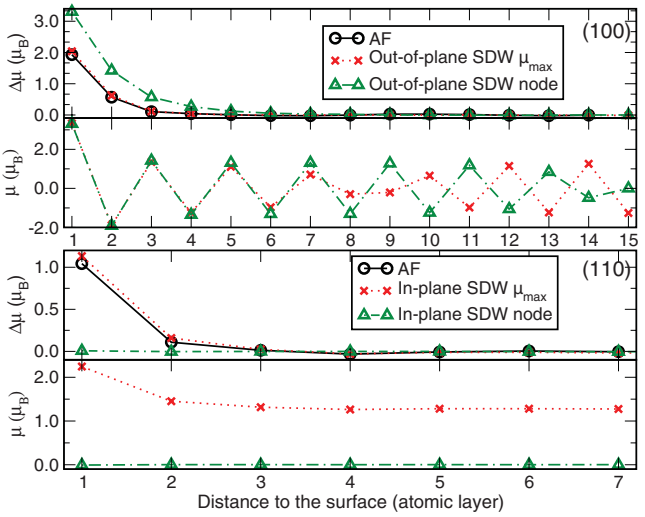

FIG. 1. (Color online) Resulting local moments (μ) near the Cr(100) and Cr(110) surfaces and the variation of their amplitudes ($\Delta\mu$) with respect to the corresponding values in the bulk. For the surfaces with SDWs, values are shown for both cases when a node and a $\mu_{\max}$ site are located at the surface (layer 1). All the results shown correspond to the same supercells as in Table I.

the instability in the NM-Cr can be significantly solved with the magnetism, it has been shown to be removed thanks to a surface reconstruction in both Mo and W.[47,48]

1. *Cr(100) with spin-density waves*

In order to achieve a more comprehensive understanding of magnetic properties near the surfaces, other magnetic structures present in bcc bulk Cr need to be considered. SDW being the most important, which has been observed experimentally near both (100) and (110) surfaces.[6–9] These

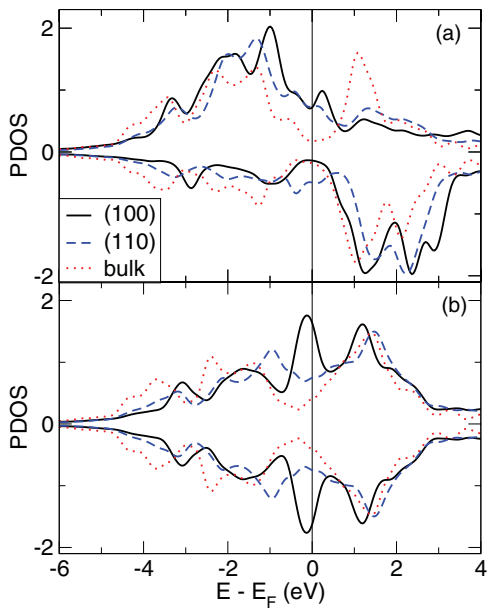

FIG. 2. (Color online) Projected density of states (in states/eV) on topmost-layer Cr atoms of the Cr(100) and the Cr(110) surfaces. The corresponding magnetic state of Cr is (a) AF and (b) NM.

findings bring two interesting questions: how may the SDW structure be modified due to the presence of the surface? And how may the interplay between SDW and surface influence their respective stability?

We focus first of all on the (100) surface, where two nonequivalent SDW orientations with respect to the surface may in principle exist, that is, either a [001] or a [010] SDW contained in the surface plane, which will be referred as an in-plane SDW, and a [100] SDW, with its wave vector perpendicular to the surface, will be called as an out-of-plane SDW. Following the available experimental data, where only the out-of-plane waves have been observed,[6,9] we have limited our present studies to these SDWs. A schematic representation of them are shown in Fig. 3(a). To consider these structures we have considered Cr slabs of 28, 56, and 84 atomic layers.

In the presence of the out-of-plane SDW, each Cr layer shows a uniform magnetization. It is therefore in agreement with the widely accepted model of topological antiferromagnetism near the Cr(100), consisting of a layered antiferromagnetism along the [100] directions.[49] Based on purely geometrical considerations, any amplitude of local magnetic moment may *a priori* be found at the surface layer. However, the various resulting magnetic structures may not be equivalent from both magnetic and energetic viewpoints. To illustrate this point, we focused on two extreme situations where a SDW node and a maximum magnetic moment site ($\mu_{\max}$) are located at the surface topmost layer.

The change of local moments amplitudes as a function of distance to the surface with respect to the corresponding bulk values are plotted in Fig. 1. It shows a zone of large local moments near the surface in both situations. Particularly in the case of the original SDW node at the surface, the local moment at the surface increases from 0 to $3.3\mu_B$ after electronic-structure relaxations, indicating the destruction of the surface node, and a local increase of SDW period. Positions of nodes at inner layers remain however unchanged.

At variance, when the SDW-$\mu_{\max}$ sites are located at the Cr(100) surface layer, the calculations reveal that the overall structure of the SDW is preserved, confirming previous DFT results.[18–20] In particular, the nearest node of the surface,

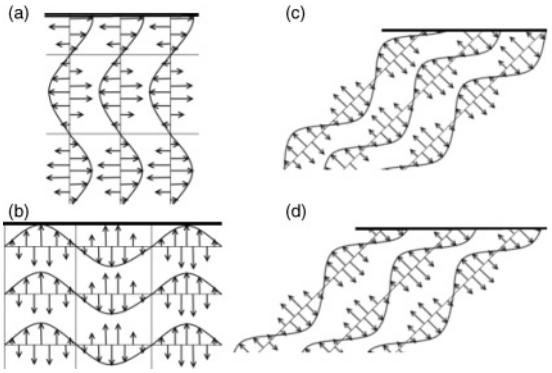

FIG. 3. Schematic representation of the different orientations of SDW near a Cr surface or its interface with Fe: (a) the out-of-plane SDW near the Cr(100) or the Fe/Cr(100), (b) the in-plane SDW, (c) the coherent, and (d) the incoherent out-of-plane SDW near the Cr(110) or the Fe/Cr(110). The surface and the interface planes are symbolized by a thick black lines.

located at the eighth layer from the surface, is practically not disturbed. The corresponding moment-amplitude increase is only $+0.03\mu_B$. Hereafter we only refer to this SDW structure when talking about out-of-plane SDWs near the Cr(100) surface.

When looking at relaxed formation energies of the Cr(100) with this SDW-Cr as given in Table I, the converged value (3.39 J/m^2) is very close to that of the AF state (3.37 J/m^2), and significantly lower than the values corresponding to the NM state. Such relative energies are found to be independent of the structural relaxations, when comparing the relaxed and unrelaxed surface energies (Table I). Also, it can be noticed that the structural relaxation effects are tiny for both the SDW and the AF cases ($\Delta E^f_{\rm surf} \lesssim 0.03$ J/m^2), and much smaller than the NM case (0.14 J/m^2). In all the three cases, that is, AF, NM, and SDW, the displacement of the surface atoms is inward during the relaxation. The corresponding reductions of the interlayer distances are -1.3%, -10.0%, and -0.5%, respectively.

On the other side, the variation of the local magnetic moments near the surface (as shown in Fig. 1) also helps to better understand the influence of the surface on the stability of the SDW structure, taking as reference the layered AF state. We observe for the SDW the same qualitative behavior as for the AF structure with the same range of magnetic perturbation due to surface, that is, the topmost five layers, besides some small quantitative differences. For instance, the corresponding magnitude of $\Delta\mu$ is slightly larger for a topmost-layer atom in the SDW state ($+2.03\mu_B$) compared to the AF state ($+1.93\mu_B$). In addition, we note from Fig. 4 that the PDOS on the topmost-layer Cr atom at both the SDW and the AF states are also very similar.

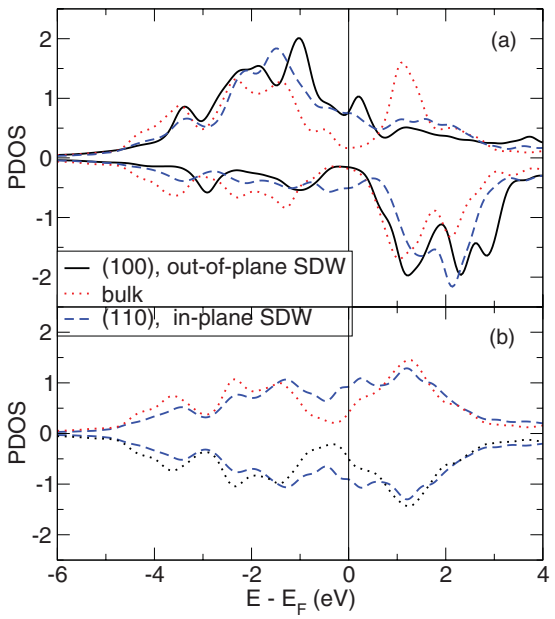

FIG. 4. (Color online) Projected density of states (in states/eV) on topmost-layer Cr atoms in the Cr(100) and the Cr(110) surfaces with respective out-of-plane and in-plane SDWs. Upper (a) and lower (b) panels show the cases when a surface Cr atom is a $\mu_{\rm max}$ site or a node of SDW, respectively.

2. *Cr(110) with spin-density waves*

Concerning the (110) surface, we also need to consider both in-plane and out-of-plane SDWs. But, at variance with the Cr(100) case, the wave vector in the latter case makes a 45° angle with the surface plane as shown in Figs. 3(c) and 3(d). Fourteen-layer slabs are used to represent the surface with the various SDW structures.

First of all, the change of local magnetic moments near the (110) surface is shown in Fig. 1 with the in-plane SDWs. Very weak magnetic influence of the (110) surface is observed. Interestingly, the nodes at the surface layer are preserved, different from the Cr(100) case. The local moment variation of a $\mu_{\rm max}$ site and a node are similar to the change observed in the AF and NM states, respectively. The little perturbed magnetic structure results as a consequence to keep phase coherence of the SDWs, which suggests that bulk influence is prevailing over surface effects in this case.

From PDOS on the topmost layer Cr atoms as plotted in Fig. 4, we also notice that it looks very similar to the PDOS shown in Fig. 2. That is, electronic modifications induced by the surface are practically the same for the AF and the SDW-$\mu_{\rm max}$ Cr atoms, as for NM and SDW-node Cr atoms.

The formation energy of (110) surface with the in-plane SDW is slightly higher than the one obtained with the AF Cr [$\Delta E^f_{\rm surf}$(SDW-AF) = 0.05 J/m^2] but lower than the one obtained with NM Cr [$\Delta E^f_{\rm surf}$(SDW-NM) = -0.14 J/m^2]. The explanation of this result is rather straightforward as the surface energies are lowered due to the magnetism, shown at the beginning of Sec. III A. The in-plane SDW containing both high-moment and low-moment sites at the surface is therefore expected to show its energy between the high-moment AF and the NM cases.

On the other side, the case of the out-of-plane [100] SDWs appears to be more complicated. Indeed, two different magnetic structures may be possible near the (110) surface [Figs. 3(c) and 3(d)], where the relative stability may strongly depend on the competition between bulk and surface influences. In the first case, the $\mu_{\rm max}$ sites of all the parallel SDWs are pinned at the surface layer, consistent with the known magnetism enhancement near a surface [Fig. 3(d)]. However, as a consequence, it induces a loss of phase coherence that SDW should exhibit in bulk Cr, in the perpendicular direction, for example, the [010]. Such a structure may be expected to be favored for very thin films where surface effect are predominant. Interestingly, it has also been evoked as a possible structure near a stepped (100) surface in a previous experiment.[9]

The second structure results from a direct cut of a perfect bcc crystal with [001] SDWs along a (110) plane, conserving thus the SDW phase coherence in, for example, the [010] direction [Fig. 3(c)]. As a consequence, some nodes of SDW are constrained to remain at the surface,[11] which has been shown to be an unstable situation at the (100) surface. In general, we may expect the coherent SDW structure to be favored for sufficient thick Cr films, where the bulk effects dominates over the surface influence.

In this work we have considered both incoherent and coherent SDW structures in order to have a clearer picture of the balance between the surface and the bulk effects. It is

worth mentioning that, in the latter case, a 45° tilted supercell with particularly large surface area of $14\sqrt{2}a_0^2$ was needed to simulate the coherent waves.

The resulting magnetic structure of incoherent SDW near Cr(110) is strongly perturbed. For instance, most nodes at subsurface and inner layers are shifted from each other, attempting to recover the phase coherence. The surface energy of Cr(110) with incoherent SDWs monotonously increases with the number of Cr layers. As expected, $E^f_{\text{surf}}(110)$ never reaches a converged value. This trend is directly linked to the bulk contribution to $E^f_{\text{surf}}(110)$, inducing an energy increase due to the loss of SDW phase coherence. We notice in particular that $E^f_{\text{surf}}(110)$ with incoherent SDWs is always much higher than $E^f_{\text{surf}}(110)$ with in-plane SDW, which tends to show a dominance of bulk influence over surface effects even for the very thin (110) films considered here.

At variance, the surface energy obtained with the coherent out-of-plane geometry is not supposed to increase with the number of Cr layers. The increasing number of inner layers are indeed composed by coherent SDWs, just as in the bulk Cr. However, our results still reveal a nonnegligible surface effect on the SDW. Before atomic-position relaxations, the SDW nodes located at topmost layer are already destroyed, similar to what happened for the (100) surface. A consequent loss of coherence occurs in the topmost layers. Then, the relaxations allows a rearrangement of magnetic structures in order to recover the phase coherence. An increase of the SDW period from $14a_0$ to about $20a_0$ therefore occurs, caused by shifts of some of the inner nodes toward the surface. We find that all the SDW nodes are destroyed within the two topmost surface layers, whereas they are preserved at inner layers. This result shows that out-of-plane SDW is not stable for very thin films of Cr as considered here. Several additional calculations with thicker Cr slabs containing at least 784 atoms will be required to better understand the stability of out-of-plane SDW, which are beyond the scope of the present study.

3. *Comparison between Cr (100) and Cr (110)*

If comparing the properties of both Cr(100) and Cr(110) with the various magnetic structures (AF, SDW, and NM), the following features are worth pointing out.

Consistent with the experimental findings, we suggest that the out-of-plane SDW with the $\mu_{\max}$ sites at the surface is the only stable SDW structure near the (100) surface. In addition, it can be said that such a magnetic structure is very weakly influenced by the presence of a (100) surface and behaves as a bulk SDW. Both magnetic and electronic structures of the surface Cr atoms are rather similar between the AF and the SDW state, which may explain the negligible surface energy difference ($0.02\ \text{J}/\text{m}^2$) between these magnetic states.

At variance, the in-plane SDW is the only stable SDW structure near the (110) surface for the slab thickness considered. Its stability near the Cr(110) is in qualitative agreement with experimental findings dealing with Cr(110) thin films from Rotenberg *et al.*[11] As suggested by the authors, a reorientation of SDWs from in-plane to out-of-plane for intermediate thickness may still be possible. This would explain why Braun *et al.* observed for thick films the dominance of out-of-plane SDWs over in-plane SDWs.[7]

Finally, the present results show that the (100) surface has a lower energy than the (110) with both SDW and AF structures, contrary to the NM case.

B. Impact of magnetism on Fe/Cr interfaces

The aim of this section is to investigate the energetics of Fe/Cr interfaces and their link with the magnetic interactions present in the system. We have thus carried out calculations considering various magnetic structures for the Cr slab keeping unchanged the standard ferromagnetic Fe structure. For comparison, we have also performed calculations on interfaces between Cr and bcc Cu, the latter being chosen as a prototype of NM full-3*d* band element. Considering that the differences of atomic volumes between Cr and both Fe and Cu are small in a bcc lattice, the objective of such a comparison is to better understand the effect of Fe-Cr magnetic coupling on the interface properties.

In the following, the formation energy of a given Fe/Cr interface (E^f_{int}) is calculated as

$$E^f_{\text{int}} = \frac{1}{2A}[E(\text{Cr}_n,\text{Fe}_m,2\text{int}) - E(\text{Cr}_n) - E(\text{Fe}_m)], \quad (2)$$

where $[E(\text{Cr}_n,\text{Fe}_m,2\text{int})]$ denotes total energy of a supercell containing n-Cr layers, m-Fe layers, and two identical interfaces. $E(\text{Cr}_n)$ and $E(\text{Fe}_m)$ are the total energies of the corresponding perfect bcc supercells containing, respectively, the same number of Fe and Cr atoms as the supercell with the interfaces. The magnetic state of the reference Fe bulk system is always the ferromagnetic, whereas it may be either the AF, the NM, or the SDW state for bulk Cr. Noncollinear magnetic structures are also considered. A is the corresponding interface area, equal to a_0^2 and $\sqrt{2}a_0^2$ for the (100) and the (110) interfaces, respectively.

The resulting values are reported in Table II.

TABLE II. Relaxed Fe/Cr interface formation energies (E^f_{int} in J/m^2) for the various Cr magnetic structures, where op-SDW, ip-SDW, and NColl denote the out-of-plane, the in-plane SDW, and the noncollinear configuration, respectively. The magnetic state of Fe is always FM. These values are converged with respect to the number of Fe and Cr layers for the AF- and NM-Cr cases with 15 layers per element, where PWSCF values are also given in parentheses. We considered 39 atomic layers of Fe and of Cr for the noncollinear (NColl) structures. The values shown correspond to $\theta = 90°$. The supercell used for Fe/Cr(100) with the op-SDW consist of 29 layers of Fe and either 42 or 70 layers of Cr. That for the Fe/Cr(110) with ip-SDWs contains 14 layers of Fe and 10 layers of Cr with 28 atoms per layer.

Cr magnetic order	AF	NM	1.5 op-SDW	2.5 op-SDW	ip-SDW	NColl
(100)	0.11 (0.14)	0.12 (0.16)	0.11	0.11	–	0.17
(110)	0.19 (0.26)	0.09 (0.14)	–	–	0.12	0.17

1. Interfaces with collinear magnetic structures

We first address the interfaces between the FM Fe and the AF Cr within a collinear-magnetism formalism. Supercells with 15 atomic layers of each element are used for such calculations. By comparing the AF-Cr and the NM-Cr cases, we notice a strong effect of magnetism on relative formation energies of interfaces. Indeed, the same as for the Cr surfaces (Sec. III A), formation energy of the (100) interface is lowered when switching from the NM to the AF Cr. On the other side, the opposite trend is observed for the (110) interface, where the interface energy increases significantly from the NM to the AF Cr. As a result, the lowest energy interface between the FM Fe and the AF Cr is the (100), whereas (110) is the lowest energy interface when considering the NM Cr. We note from Table II that despite some small discrepancies between the SIESTA and the PWSCF values, such a trend is common to both DFT approaches. Also, we have verified that atomic-position relaxation is negligible compared with the surface case. These energetic trends remain unchanged before and after the structural optimization.

The present prediction with the AF-Cr state is also consistent with a previous DFT data evaluating the adhesion energies of the same (100) and (110) Fe/Cr interfaces.[33] On the other side, the energies seems to differ from the case with very few Fe and Cr layers, where residual interaction may exist between the two interfaces in the same simulation cell. For instance, Lu *et al.*[34] found a slightly higher interface energy for the (100) than for the (110), when considering relatively small supercells, that is, with no more than five atomic layers of each element.

Similar to the Cr surface case, this anisotropy of interface energies is not expected regarding the usual trend of interfaces between the bcc metals with phase separation tendency, where the densest interface, that is, the (110), shows to be the lowest in energy. In the Fe/Cr interface case, such a behavior is mainly caused by Fe-Cr magnetic coupling. Indeed, significant magnetic frustrations occur near the (110) interface due to the atomic configuration at the interfacial layers as shown in Fig. 5, that is, the first- and second-nearest neighbor (1nn and 2nn) Fe-Cr antiparallel coupling tendencies predicted previously[4,50,51] are in conflict with the FM and AF order in respective bulk Fe and Cr. This frustration induces a decrease of magnetic moments on both Fe ($\Delta\mu_{\mathrm{Fe}} = -0.25\mu_B$) and Cr ($\Delta\mu_{\mathrm{Cr}} = -0.33\mu_B$) atoms near the (110) interface (Fig. 6) which has also been observed experimentally.[32] Consistently it is also expected to be at the origin of the high value of the (110) interfacial energy.

On the other hand, we note from Fig. 5 that the 1nn Fe-Cr magnetic frustration does not exist for the (100) interface, but the 2nn frustration remains. Indeed, the magnetic profile of Fig. 6 shows only a small reduction of magnetic moments on the subinterface Cr ($\Delta\mu_{\mathrm{Cr}} = -0.13\mu_B$) and the interface Fe ($\Delta\mu_{\mathrm{Fe}} = -0.09\mu_B$) atoms which are 2nn of each other. This frustration seems to have little impact on the energetics of the (100) interface, since its interface energy decrease from the NM to the AF Cr state, opposite to the (110) interface behavior.

The statement of a magnetic driving force inducing an unusual anisotropy of interface energies is also supported by a comparison with the corresponding Cu/Cr interface, whose formation energy is reported in Table III. Indeed, as Cu always remains nonmagnetic, we suppress any kind of magnetic

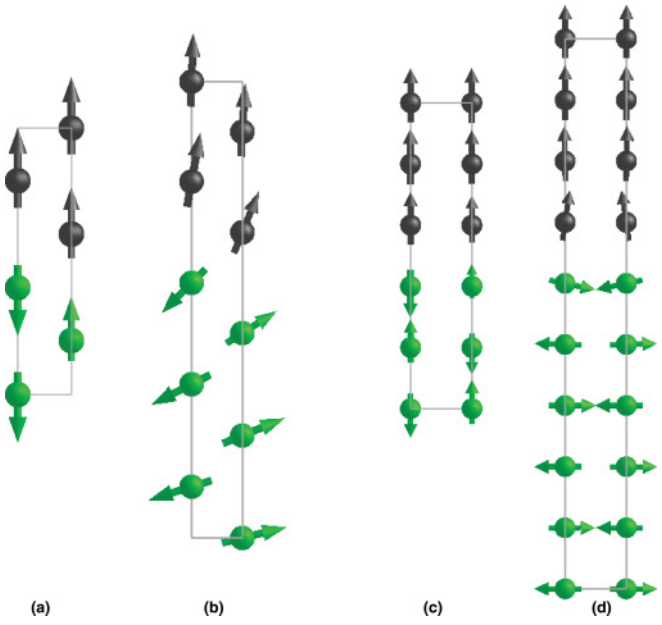

FIG. 5. (Color online) Schematic side views of the Fe/Cr(100) interface with (a) collinear and (b) noncollinear magnetic structures. The same representations for the (110) interface are shown in (c) and (d), respectively. Fe atoms are symbolized by black balls and Cr atoms by green (light gray) balls. The orientations and amplitudes of local magnetic moments are indicated by the arrows.

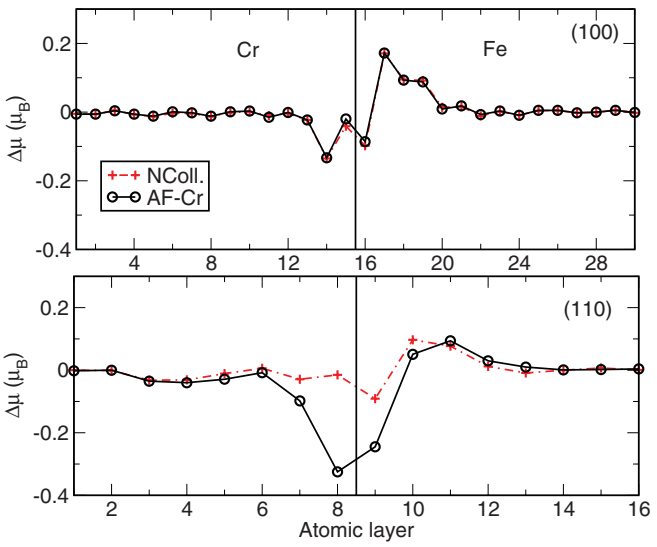

FIG. 6. (Color online) Variation of Cr and Fe local moments magnitude (in μ_B) around the (100) and (110) Fe/Cr interfaces with respect to their respective bulk values ($2.25\mu_B$ for FM-Fe and $1.39\mu_B$ for AF-Cr). The results shown for both collinear (AF-Cr) and noncollinear structures correspond to the same supercells as in Table II. Interfaces are symbolized by verticals lines. Note that for the (110) interface, only the most frustrated Cr atoms (the right column of Fig. 5) are represented.

TABLE III. Relaxed Cu/Cr interface formation energies E_{int}^{f} (J/m^2) with Cr at either AF or NM states. The magnetic state of Cu is always NM. These values are converged with respect to the number of Cu and Cr layers, both equal to 15.

Cr magnetic order	AF	NM
(100)	0.88	1.26
(110)	0.79	1.05

frustration present at the Fe/Cr interfaces. Our calculations show, as expected, that the (110) interface is the energetically preferred one for both AF and NM Cr states. Consistently all the magnetic moment reductions identified for the Fe/Cr interface have disappeared for the Cu/Cr interfaces.

Now we turn to compare, from an electronic viewpoint, the (100) and the (110) interfaces. It is interesting to note from Fig. 7 that the PDOS of the majority-spin band on a interfacial-layer Cr atom around the Fermi level is clearly large for the Fe/Cr(110) interface with the AF-Cr state, compared with the Fe/Cr(100) and the Cr bulk. Such a high PDOS is significantly reduced when considering the NM-Cr state, when any magnetic coupling and frustration is removed. At variance the PDOS of interfacial-layer Cr atoms at the interfaces with Cu are expectedly very similar to the PDOS at the corresponding Cr surfaces (Fig. 8). In particular, the larger Fermi-level PDOS on the Cu/Cr(100) interface for the NM-Cr than for the AF-Cr case may be consistent with a higher energy difference between Cu/Cr(100) and Cu/Cr(110) interfaces for the NM-Cr case (Table III).

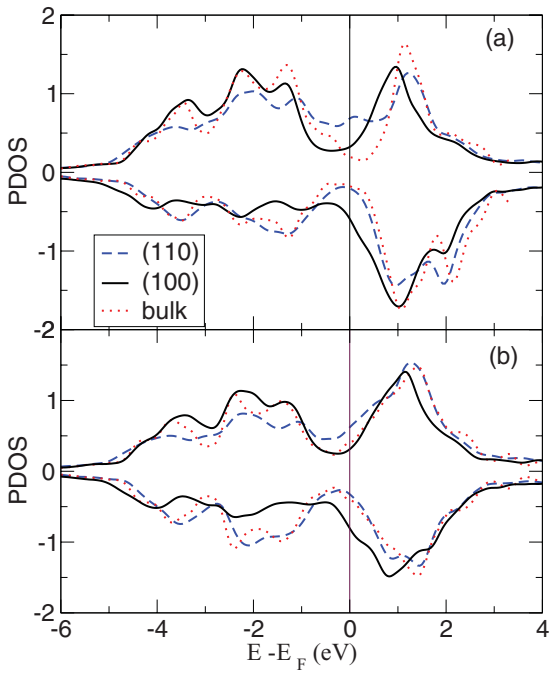

FIG. 7. (Color online) Projected density of states (in states/eV) on the interfacial-layer Cr atoms of Fe/Cr(100) and Fe/Cr(110). The magnetic state of Cr is either (a) AF or (b) NM, whereas the magnetic state of Fe remains FM.

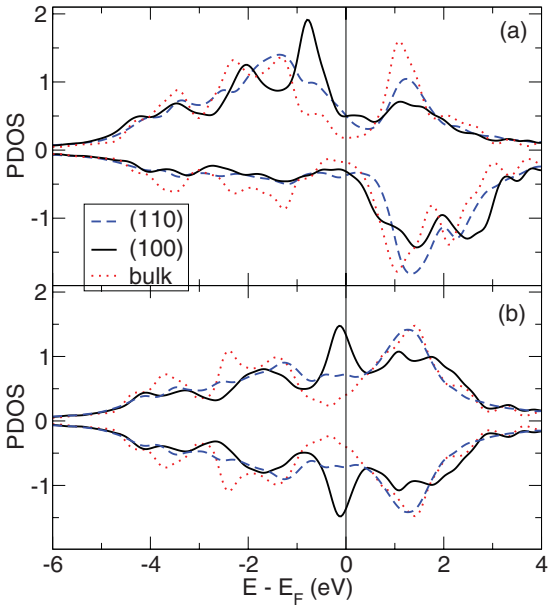

FIG. 8. (Color online) Projected density of states (in states/eV) on the interfacial-layer Cr atoms of Cu/Cr(100) and Cu/Cr(110). The magnetic state of Cr is either (a) AF or (b) NM, whereas Cu is always nonmagnetic.

The above studies on the Fe/Cr and Cu/Cr interfaces clearly establish the dominant role of Fe-Cr magnetic coupling on the relative stability of Fe/Cr interfaces. Nevertheless, this conclusion is derived from calculations with a simplified representation of the Cr magnetic structure and within a collinear magnetism approach. Below we aim to gain a deeper insight considering more realistic magnetic structures. In particular, to see how the identified Fe-Cr magnetic frustrations could be solved around the Fe/Cr interfaces.

2. Interfaces with noncollinear magnetic structures

One way to partly relax the magnetic frustration is to go beyond the collinear constraint. Indeed, Fe and Cr have been shown experimentally to be perpendicularly coupled near a (110) interface. This perpendicular coupling may be preserved even when Fe magnetization axis is rotated using an external magnetic field.[25,26] Such type of noncollinear coupling may in principle result from two phenomena: spin-orbit interaction, which goes beyond the purpose of this paper, and geometrical relaxation of magnetic frustration. We have explored the presence of possible noncollinear structures for the Fe/Cr(100) and the Fe/Cr(110) interfaces purely driven by the magnetic frustrations. Supercells containing 39 atomic layers of each element have been used to ensure the convergence of the resulting magnetic structures and the interface energies. We have in fact found various local energy minima corresponding to different angles (θ) between magnetic moments of the inner Cr and Fe atoms for each case (Fig. 9). Schematic representation of structures with $\theta = 90^\circ$ are shown in Fig. 5, with the corresponding interface energies listed in Table II.

For the (110) interface, the lowest energy corresponds to $\theta = 90^\circ$. Our results confirm that this noncollinear structure causes an energy decrease of 0.02 J/m^2 with respect to the collinear (AF-Cr) case, while some other intermediate

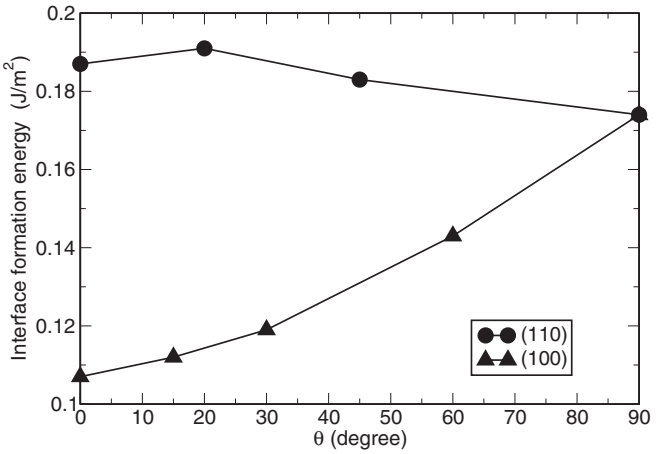

FIG. 9. Interface formation energy as a function of the angle θ between local magnetic moments of Cr atoms at an inner layer and of Fe, where $\theta = 0^\circ$ represents the collinear configuration. Values are shown for both Fe/Cr(100) and Fe/Cr(110) interfaces.

angles lead to higher energy states. The magnetic moments of practically all the Fe and the Cr atoms are thus perpendicular to each other, in good agreement with experiments. Only slight angle deviations are found for the interface-layer atoms. We obtain angles of 8° and 12°, respectively, for these Fe and Cr atoms with regard to perfect perpendicular coupling. This slightly perturbed geometry is actually an optimal compromise to satisfy simultaneously the Fe-Fe, Cr-Cr, and Fe-Cr couplings mentioned above. The moment-magnitude profile from Fig. 6 also allows us to confirm the relaxation of magnetic frustration. We observe that the local magnetic moments of interfacial Cr and Fe atoms, strongly reduced in the collinear configuration, are becoming significantly closer to their respective bulk values in the noncollinear structures.

Concerning the (100) interface, we have to determine if the 2nn Fe-Cr frustration alone, mentioned in Sec. III B 1, is a strong enough driving force to induce noncollinear magnetic structures. Such structures have been observed experimentally with a perpendicular coupling of Fe and Cr moments,[22] but their origin was rather attributed to the magnetic frustration caused by interdiffusion at the topmost layers of the interfaces, at variance with the Fe/Cr(110) case. Some previous theoretical works using semiempirical models also pointed out that such defective interfaces may induce noncollinear structures near Fe/Cr(100).[35–41] Consistently our calculations indicate that noncollinear structures can only be found as metastable states for perfect (100) interfaces with higher energies than the collinear configuration (Table II).

The corresponding magnetic structures show a gradual variation of the Cr moments direction before converging to a precise θ angle with respect to the Fe moments for inner Cr atoms. We have verified that, at variance with the (110) interface, the resulting interfacial energy increases monotonously from $\theta = 0^\circ$ (collinear) to 90°, the latter being the highest energy case (Fig. 9). Figure 5 shows the case for $\theta = 90^\circ$ in order to compare with the (110) interface. Please note that in the collinear configuration (Fig. 5), the (100) interface shows only one frustrated 2nn Fe-Cr pair per Cr atom compared to four nonfrustrated Fe-Cr 1nn couplings. On the other side, even though the 2nn frustration can be partly solved in the noncollinear configuration, the perfect antiparallel coupling of the 1nn Fe-Cr pairs are however perturbed. As a consequence, the energy decrease connected to the 2nn interaction may be "overcompensated" by the creation of the additional frustrations. This explains why the noncollinear structure results to be only metastable. Figure 6 also indicates that the reduction of local-moments magnitude near the interface cannot be recovered when removing the collinear constraint.

3. Interfaces with spin-density waves

The studies carried out in Secs. III B 1 and III B 2 have certainly not captured all the magnetic complexity of Cr. As for the Cr surfaces, a discussion including the SDW structure near the Fe/Cr interface is particularly required.

Close to a (100) interface, we decided, in view of existing experimental results,[52] to consider only the out-of-plane SDWs. Please note that at variance with several previous theoretical works mentioned in Sec. I, our interest is focused on the magnetic structure at the Fe/Cr interface itself rather than the Fe/Cr multilayers. We have therefore considered thick enough Cr and Fe slabs to ensure that the magnetic and energetic properties of the interfaces are well converged. Due to the periodic boundary conditions imposed by our bicrystal approach, we have considered half-periods of SDW, that is, 42 and 70 Cr-atomic layers corresponding, respectively, to 1.5 and 2.5 wave periods. In this way we ensure the interfacial Fe-Cr magnetic coupling to be antiparallel at both interfaces to minimize magnetic frustrations.

For the out-of-plane SDWs with either a node or a low-moment site located at the interface, we have always noticed, as expected, an increase of Cr local moment at the interface with respect to the corresponding site in the bulk (Fig. 10). It is induced by the antiparallel Fe-Cr magnetic coupling at the interface, similar to the situation with isolated Cr atoms in bulk Fe.[50] This moment-magnitude increase indicates a qualitative suppression of the interfacial SDW nodes, inducing a local increase of SDW period in the case where the original SDW has an interfacial node.

Now, turning to consider the (100) interface with the $\mu_{\max}$ sites at the interface layer, we reported in Table II the corresponding formation energies. which shows to be already converged for the 1.5-periods case (42 Cr layers). When looking at the detailed interfacial magnetic structure, we observe a decrease of local moments magnitude at the near-interface Cr layers with respect to the original SDW (Fig. 10). A particularly strong moment reduction of the subinterfacial Cr atom, caused by the 2nn Fe-Cr magnetic frustration, still remains as in both the AF and the noncollinear Cr cases. It suggests that, like the noncollinear structure, this SDW structure does not help to solve such a magnetic frustration either. Besides these changes, all the nodes in the Cr slab are preserved, in agreement with previous calculations showing a relatively limited impact range of the Fe/Cr interface on the magnetic structure of Cr.[29]

For the (110) interface, we have considered again the two different SDW orientations, that is, the in-plane and the

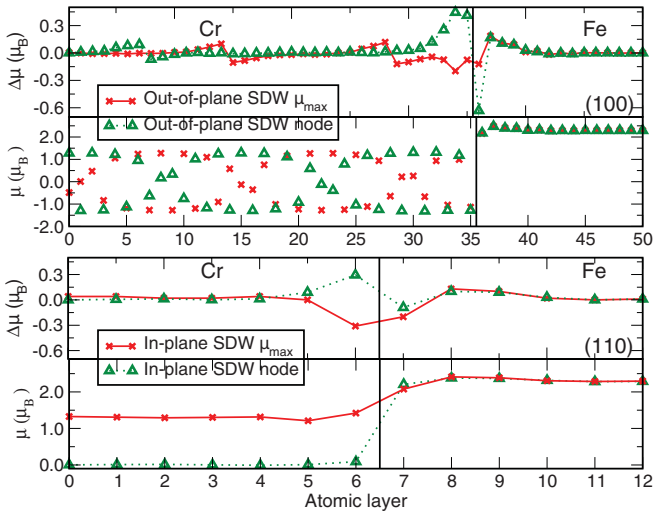

FIG. 10. (Color online) Resulting local moments of Cr and Fe (μ) around the Fe/Cr(100) and Fe/Cr(110) interfaces with SDWs and the variation of their amplitudes ($\Delta\mu$) with respect to the corresponding bulk values. The values are obtained with the same supercells as in Table II. Interfaces are symbolized by vertical lines. The both cases where a SDW node and a $\mu_{\max}$ site are located at the interfacial layer are shown.

out-of-plane. The simulation supercells contain 14 atomic layers of Fe and, respectively, 10 and 14 layers of Cr in order to fulfill different geometric requirements.

Considering first of all the unrelaxed structure of the coherent out-of-plane SDW, we observe an increase of magnetic moments of nodes located at the interface layer ($\Delta\mu = +0.98\mu_B$). Although this increase is lower than for the (110) surface ($\Delta\mu = 1.76\mu_B$), it still means a clear suppression of the interfacial nodes. The atomic-position relaxations cause, as for the Cr(110) surface, an increase of the SDW period from $14a_0$ to $20a_0$. This SDW structure is therefore not stable near a Fe/Cr(110) interface.

On the other side, the structure of an in-plane SDW is preserved at the Fe/Cr(110) interface. Based on the variations of local magnetic moments near the interface on both Cr and Fe sides (Fig. 10), we note that the magnetic moment decrease coming from Fe-Cr 1nn magnetic frustration is still present around an interfacial $\mu_{\max}$ site. However, the corresponding moment decrease is recovered around an interfacial node. This latter indicates that the Fe-Cr 1nn magnetic frustration can be periodically relaxed along the interface near each node site.

The corresponding PDOS on the Cr interface layer atoms located at node and $\mu_{\max}$ site of SDW are very close to the PDOS of, respectively, NM and AF interface layer Cr atoms. It confirms that the in-plane SDW is practically not influenced by the Fe/Cr(110) interface.

Finally, considering all the studied cases allows an overall description of interface energies as a function of Cr magnetic structure (Table II).

Regarding the (100) interface, the formation energies found are the same for both AF and out-of-plane SDW magnetic structures. They are clearly smaller than the values obtained for any noncollinear configuration and the NM-Cr case.

For the (110) interface, its formation energy is lower with the in-plane SDW compared to the AF Cr, at variance with the Cr(110) surface. This result is linked to the presence of node sites at an interface that relaxes locally the magnetic frustration around the (110) interface. The presence of nodes has also been mentioned in previous works considering Fe/Cr(100) interfaces with roughness.[53] We have thus identified two possible ways to relax the Fe-Cr 1nn and 2nn magnetic frustrations that occur at the (110) interface. From our calculations, the energy decrease due to the presence of the in-plane SDW [ΔE(AF-SDW) $= -0.07\,\mathrm{J/m^2}$] is even larger than that caused by the noncollinear structure [ΔE(AF-NColl) $= -0.02\,\mathrm{J/m^2}$].

It is work mentioning that we have not found any inversion of the relative energy between the (110) and the (100) Fe/Cr interfaces for all the considered magnetic structures. The (100) remains the lowest energy interface. Even though it is out of the scope of the present study, we might expect that a combination of the two magnetic structures, that is, noncollinear SDW, may also occur in order to further lower the energy of the Fe/Cr(110) interface.

IV. CONCLUSIONS

The aim of this work is to investigate, by means of DFT calculations, the interplay between magnetic structure of Cr and two types of extended defects, that is, low index Cr surfaces and the corresponding interfaces with FM-Fe.

Concerning Cr surfaces, we confirm the role of magnetism to lower the surface energy of Cr(100) with respect to Cr(110), opposite to the same surfaces with NM-Cr. When considering as explicitly as possible the magnetic ground state of Cr, the SDW state, near the surfaces, we have shown that the resulting magnetic structure is strongly dictated by the surface orientation. For instance, among all the possible orientations of the wave vector, only the out-of-plane SDWs may be stable near the Cr(100) surfaces. Consistent with previous experimental and theoretical studies, their structure is overall preserved with the high-moment sites located at the surface layer.

At variance, the in-plane SDWs are suggested to be the most stable ones for very thin Cr(110) films as considered here, consistent with existing experimental data. Their relative stability with respect to the coherent out-of-plane waves, experimentally observed for thicker films, is expected to be determined by a subtle balance between surface and bulk influences. Further systematic DFT calculations with large supercells beyond the scope of this work are required in order to identify a possible reorientation of SDW as a function of film thickness suggested by experiments.

Concerning Fe/Cr interfaces, magnetic frustrations have been identified to be responsible for a higher formation energy of Fe/Cr(110) compared to that of Fe/Cr(100). This unusual anisotropy of interface energies has been shown to be clearly different from the corresponding interfaces between Cr and a nonmagnetic element (Cu). Indeed, the (110) interface is submitted to interfacial Fe-Cr 1nn and 2nn frustrations that significantly increase its energy, whereas the (100) interface only suffers from a relatively weaker Fe-Cr 2nn frustration that has little impact on the energetics.

Two ways have been suggested to partially relax the magnetic frustrations in the (110) interface. On one side we have shown that noncollinear configurations which allow us to reach a compromise between the various Fe-Cr, Fe-Fe, and Cr-Cr magnetic couplings can lower the interface energy. As a result, local moments of inner Fe and Cr atoms are perpendicular to each other, in excellent agreement with experimental data. On the other side, in-plane SDWs show very stable magnetic structures with the nodes at the interface layer, driven by the tendency to preserve phase coherence as in bulk Cr. The presence of low-moment sites at Fe/Cr(110) also helps to periodically relax the magnetic frustrations and lower the interfacial energy. Based on the present results, we may expect that, as a combination of the two structures, noncollinear SDW may also be present near the Fe/Cr(110) interface, contributing to further lower its formation energy. Additional DFT calculations beyond the present study are required to confirm this hypothesis.

Regarding the Fe/Cr(100) interface, the Fe-Cr 2nn magnetic frustration shows not to be strong enough to stabilize noncollinear structures, which are only metastable states. Otherwise, similar to the Cr(100) surfaces, the out-of-plane SDWs with the high-moment sites at the interface layer are confirmed to be the only stable SDW orientation around the Fe/Cr(100) interfaces.

ACKNOWLEDGMENTS

This work was performed using HPC resources from GENCI-CINES (Grant Nos. 2010-x2010096020 and 2011-x2011096020).

[1] L. Corliss, J. Hastings, and R. Weiss, Phys. Rev. Lett. **3**, 211 (1959).
[2] V. Bykov, V. Golovkin, N. Ageev, V. Levdik, and S. Vinogradov, Dokl. Akad. Nauk SSSR **4**, 1149 (1959).
[3] E. Fawcett, Rev. Mod. Phy. **60**, 209 (1988).
[4] R. Soulairol, C.-C. Fu, and C. Barreteau, Phys. Rev. B **83**, 214103 (2011).
[5] J. P. Hill, G. Helgesen, and D. Gibbs, Phys. Rev. B **51**, 10336 (1995).
[6] P. Sonntag, P. Bodeker, A. Schreyer, H. Zabel, K. Hamacher, and H. Kaiser, J. Magn. Magn. Mater. **183**, 5 (1998).
[7] K. F. Braun, S. Folsch, G. Meyer, and K. H. Rieder, Phys. Rev. Lett. **85**, 3500 (2000).
[8] M. Kleiber, M. Bode, R. Ravlic, N. Tezuka, and R. Wiesendanger, J. Magn. Magn. Mater. **240**, 64 (2002).
[9] T. Hanke, S. Krause, L. Berbil-Bautista, M. Bode, R. Wiesendanger, V. Wagner, D. Lott, and A. Schreyer, Phys. Rev. B **71**, 184407 (2005).
[10] B. Santos, J. M. Puerta, J. I. Cerda, R. Stumpf, K. von Bergmann, R. Wiesendanger, M. Bode, K. F. McCarty, and J. de la Figuera, New J. Phys. **10**, 013005 (2008).
[11] E. Rotenberg, B. Freelon, H. Koh, A. Bostwick, K. Rossnagel, A. Schmid, and S. Kevan, New J. Phys. **7**, 114 (2005).
[12] J. Meersschaut, J. Dekoster, S. Demuynck, S. Cottenier, B. Swinnen, and M. Rots, J. Magn. Magn. Mater. **198-199**, 641 (1999).
[13] J. Meersschaut, J. Dekoster, R. Schad, P. Belien, and M. Rots, Phys. Rev. Lett. **75**, 1638 (1995).
[14] R. Hafner, D. Spisak, R. Lorenz, and J. Hafner, Phys. Rev. B **65**, 184432 (2002).
[15] S. Cottenier, B. De Vries, J. Meersschaut, and M. Rots, J. Phys. Condens. Matter **14**, 3275 (2002).
[16] T. Ossowski and A. Kiejna, Surf. Sci. **602**, 517 (2008).
[17] M. Alden, H. Skriver, S. Mirbt, and B. Johansson, Surf. Sci. **315**, 157 (1994).
[18] H. Zabel, J. Phys. Condens. Matter **11**, 9303 (1999).
[19] A. M. N. Niklasson, J. M. Wills, and L. Nordstrom, Phys. Rev. B **63**, 104417 (2001).
[20] G. Bihlmayer, T. Asada, and S. Blugel, Phys. Rev. B **62**, 11937 (2000).
[21] T. Ossowski, E. Wachowicz, and A. Kiejna, J. Phys. Condens. Matter **21**, 485002 (2009).
[22] P. Bodeker, A. Hucht, A. Schreyer, J. Borchers, F. Guthoff, and H. Zabel, Phys. Rev. Lett. **81**, 914 (1998).
[23] A. Schreyer, C. F. Majkrzak, T. Zeidler, T. Schmitte, P. Bodeker, K. Theis-Brohl, A. Abromeit, J. A. Dura, and T. Watanabe, Phys. Rev. Lett. **79**, 4914 (1997).
[24] R. Fishman, J. Phys. Condens. Matter **13**, R235 (2001).
[25] H. Fritzsche, J. Hauschild, A. Hoser, S. Bonn, and J. Klenke, Europhys. Lett. **49**, 507 (2000).
[26] H. Fritzsche, S. Bonn, J. Hauschild, J. Klenke, K. Prokes, and G. J. McIntyre, Phys. Rev. B **65**, 144408 (2002).
[27] K. Hirai, Phys. Rev. B **59**, R6612 (1999).
[28] E. E. Fullerton, J. L. Robertson, A. R. E. Prinsloo, H. L. Alberts, and S. D. Bader, Phys. Rev. Lett. **91**, 237201 (2003).
[29] A. M. N. Niklasson, B. Johansson, and L. Nordstrom, Phys. Rev. Lett. **82**, 4544 (1999).
[30] I. Mirebeau, M. Hennion, and G. Parette, Phys. Rev. Lett. **53**, 687 (1984).
[31] I. Mirebeau and G. Parette, Phys. Rev. B **82**, 104203 (2010).
[32] N. Jiko, M. Almokhtar, K. Mibu, and T. Shinjo, J. Phys. Condens. Matter **17**, 2477 (2005).
[33] D. F. Johnson, D. E. Jiang, and E. A. Carter, Surface Science **601**, 699 (2007).
[34] S. Lu, Q.-M. Hu, R. Yang, B. Johansson, and L. Vitos, Phys. Rev. B **82**, 195103 (2010).
[35] D. Stoeffler and F. Gautier, J. Magn. Magn. Mater. **147**, 260 (1995).
[36] E. Martinez, R. Robles, D. Stoeffler, and A. Vega, Phys. Rev. B **74**, 184435 (2006).
[37] R. Robles, E. Martinez, D. Stoeffler, and A. Vega, Phys. Rev. B **68**, 094413 (2003).
[38] D. Stoeffler and C. Cornea, J. Magn. Magn. Mater. **240**, 223 (2002).
[39] V. Uzdin, N. Yartseva, and S. Yartsev, J. Magn. Magn. Mater. **196**, 70 (1999).
[40] V. Uzdin, A. Mokrani, C. Demangeat, and N. Yartseva, J. Magn. Magn. Mater. **199**, 471 (1999).
[41] N. Yartseva, S. Yartsev, V. Uzdin, and C. Demangeat, Comp. Mater. Sci. **17**, 468 (2000).

[42]J. Soler, E. Artacho, J. Gale, A. Garcia, J. Junquera, P. Ordejón, and D. Sanchez-Portal, J. Phys. Condens. Matter **14**, 2745 (2002).
[43]R. Soulairol, C.-C. Fu, and C. Barreteau, J. Phys. Condens. Matter **22**, 295502 (2010).
[44]V. García-Suárez, C. Newman, C. Lambert, J. Pruneda, and J. Ferrer, J. Phys. Condens. Matter **16**, 5453 (2004).
[45]F. Soisson and C.-C. Fu, Phys. Rev. B **76**, 214102 (2007).
[46]P. Giannozzi *et al*., J. Phys. Condens. Matter **21**, 395502 (2009) [http://www.quantum-espresso.org].
[47]H.-J. Ernst, E. Hulpke, and J. P. Toennies, Phys. Rev. B **46**, 16081 (1992).
[48]R. S. Daley, T. E. Felter, M. L. Hildner, and P. J. Estrup, Phys. Rev. Lett. **70**, 1295 (1993).
[49]S. Blügel, D. Pescia, and P. H. Dederichs, Phys. Rev. B **39**, 1392 (1989).
[50]T. P. C. Klaver, R. Drautz, and M. W. Finnis, Phys. Rev. B **74**, 094435 (2006).
[51]M. Y. Lavrentiev, D. Nguyen-Manh, and S. L. Dudarev, Phys. Rev. B **81**, 184202 (2010).
[52]E. E. Fullerton, S. D. Bader, and J. L. Robertson, Phys. Rev. Lett. **77**, 1382 (1996).
[53]D. I. Pierce, J. Unguris, R. J. Celotta, and M. D. Stiles, J. Magn. Magn. Mater. **200**, 290 (1999).